

SUPPRESSION AGENT VAPOR LOADING AND EFFECTIVENESS ASSESSMENT FOR ENGINE NACELLES

James W. Fleming
Navy Technology Center for Safety and Survivability
Combustion Dynamics Section, Code 6185, Naval Research Laboratory
Washington, DC 20375-5342 USA, Tel: 202-767-2065; Fax 202-767-1716
fleming@code6185.nrl.navy.mil

and

Jiann C. Yang
Fire Metrology Group, MS- 8662
National Institute of Standards and Technology (NIST), Gaithersburg, MD 20899-8662 USA
Tel: 301-975-6662; Fax: 301-975-4052; jiann.yang@nist.gov

INTRODUCTION

There is a high probability that gases or liquids with high boiling points, higher than that of Halon 1301, will be required to provide fire protection in engine nacelles. In such complex flow environments, the performance of the suppression agent will depend on a number of parameters including physical properties of the agent (heat capacity, boiling point, heat of vaporization), the application temperature, and the flow-imposed time constraints for liquid agent evaporation. This work addresses the potential performance of possible compounds via a computational approach in order to eliminate unsuitable compounds from consideration and determine favorable properties that successful agents are likely to possess.

BACKGROUND

The physics controlling the release of a liquid under pressure through an orifice and subsequent evaporation were briefly reviewed in the HOTWC 2004 paper [1]. The two processes, flash vaporization and evaporation, occur in two stages and on very different time scales. If flash vaporization occurs (agent must be discharged into surroundings at a higher temperature than its boiling point), the process is essentially instantaneous. Evaporation of any remaining liquid takes place on a much longer time scale. Both processes depend on the agent thermophysical properties (agent boiling point, heat capacity, and enthalpy of vaporization) and the environmental conditions into which the agent is released (e.g., ambient temperature, ambient vapor loading, flowfield mixing details).

The amount of a superheated liquid (gas under pressure stored at a temperature above its boiling point) that can flash vaporize after release into air versus the amount of liquid left behind can be estimated from the Jakob Number, Ja . Ja can be evaluated from the ratio of the enthalpy change required to take the liquid from its normal boiling point to the ambient temperature (sensible enthalpy) and the heat of vaporization of the liquid. Ja is not a constant but depends on the temperature of the ambient surroundings (typically air) into which the agent is discharged. Values for Ja vary from 0 to 1. A Ja near one implies that most of the agent can vaporize

immediately upon discharge. A Ja of zero characterizes compounds discharged into surroundings at a temperature equal to or lower than their boiling point. For compounds and conditions where $Ja = 0$, all of the agent released into the nacelle will be in the liquid state. Vapor production from the liquid must now rely on evaporation, a much slower process achieved by extracting heat from the surrounding air and boundaries.

In general, higher evaporation rates are favored by smaller drops and large evaporation constants (i.e., lower boiling points, smaller heats of vaporization, and **low** heat capacities). However, more agent will start out in the vapor phase (flash vaporize) for compounds with **high** heat capacity relative to the heat of vaporization. Boiling points that are low compared to the ambient conditions will always result in higher vapor concentrations in shorter periods of time. Agent vapor loading when the agent boiling point is close to or higher than the ambient air temperature depends not only on the agent properties, but also on the application conditions. In these cases, the system dynamics must also be considered in order to estimate vapor loadings.

FIRE DYNAMICS SIMULATOR

In this study, agent drop transport and evaporation in a simulated engine nacelle are treated using the NIST Fire Dynamics Simulator (FDS) version 4. The Fire Dynamics Simulator (FDS) is a computational fluid dynamics (CFD) computer code developed by NIST to study fire dynamics, smoke movement, and sprinkler-fire interaction [2]. We used FDS to model the dispersion of low boiling-point (CF_3I , $-22\text{ }^\circ\text{C}$) and high boiling-point (CF_2Br_2 , $22.9\text{ }^\circ\text{C}$) agents in a simulated engine nacelle using the existing sprinkler algorithm in FDS. Because FDS is based on the Cartesian coordinate system, a square engine nacelle was used in the simulation. The nacelle is $2.000\text{ m} \times 0.798\text{ m} \times 0.798\text{ m}$ and has the geometrical attributes (same cross section, length, and complexity) commensurate with the experimental engine nacelle fixture (ELEFANT) used to study low temperature dispersion of agent [3]. Figure 1 is a schematic of the nacelle. The inner rectangular block represents the engine core. There are two baffles attached to the inside surface of the outer block and two attached to the outside surface of the inner block. Two horizontal ribs with the same height as the baffles are placed on the outer surface of the inner core of the nacelle between the inner forward and aft baffles. The agent discharge ports are located upstream of the nacelle. Air flows in the region between the inner block and the external casing. The front and aft ports represent the corresponding measurement locations in the experimental engine nacelle test fixture.

In the simulation, the agent discharge ports were represented by two liquid sprays, one pointing vertically upward and one pointing vertically downward. The configuration is similar to the vertical tee used to discharge the agent from the bottle in ELEFANT experiments. The average liquid discharge rates through the nozzles were estimated based on typical experimental values obtained from the discharge tests. The discharge time of the agent was used as the duration of spray activation in the simulation. This time was varied according to the bottle conditions. Other spray parameters used in the simulations were assigned, or their default values were used. For example, the drop size distribution used in the simulations was in the form of a Rosin-Rammler/log-normal distribution with a median volumetric diameter of $20\text{ }\mu\text{m}$ with the distribution parameter set at 2.4 (default value used in FDS). The minimum spray angle was set at 30° and the maximum at 75° . The droplet speed at the nozzle varied from 16 m/s to 20 m/s

depending on the bottle conditions. Air speed at the inlet of the nacelle was set at 4.25 m/s, which was used in the laboratory experiments. The sprays were activated at 1.0 s from the start of FDS simulation and then de-activated at 1.2 s or 1.24 s. The dispersion process was simulated to 2 s or 3 s with $30 \times 150 \times 30$ grid cells. Liquid drop interaction with nacelle walls was handled in the way described in FDS. When a drop impacts a solid horizontal surface, it is assigned a random horizontal direction and moves at a fixed horizontal velocity component until it reaches the edge, where it drops straight down at the same fixed velocity. When the drop hits a solid surface vertically, it is removed from the computational domain. There is no heat transfer between the droplets and the boundaries. Table 1 summarizes the conditions used in the simulations.

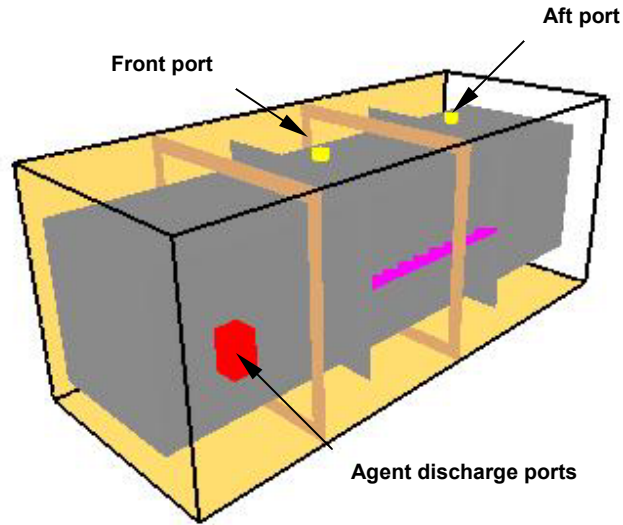


Figure 1. Engine nacelle simulator.

Table 1. Summary of conditions used in the simulation.

Agent	Nacelle & airflow temperature	Agent discharge temperature	Agent discharge rate (L/min)	Agent drop speed at discharge (m/s)
CF ₃ I	22 °C	22 °C	142	20
CF ₃ I	-40 °C	22 °C	142	20
CF ₃ I	-40 °C	-40 °C	119	16
CF ₃ I	22 °C	-40 °C	119	16
CF ₂ Br ₂ *	22 °C	22 °C	142	20
CF ₂ Br ₂	0 °C	22 °C	142	20
CF ₂ Br ₂ *	0 °C	0 °C	138	19
CF ₂ Br ₂	22 °C	0 °C	138	19

* Simulations using 200 μm and 500 μm median drop sizes were also run.

In line with the ELEFANT experiments, the dispersion effectiveness of liquid agent at various conditions was assessed based upon agent vapor concentration measurements at the front and aft

ports. The intent of this work was to evaluate vapor loading that could be attained at these two locations as a result of liquid agent evaporation under various ambient conditions.

SIMULATION OF AGENT RELEASE IN AN ENCLOSURE

A FORTRAN program was written to model the behavior of the flashing/evaporating liquid in order to gain insight into the general behavior of the released agent as well as aid in the interpretation of the FDS results. The program predicts the vapor concentration expected from an agent released into a 0.7-L box, representing the open space inside the nacelle. The liquid remaining after flash vaporization is assumed to be distributed in a log normal distribution about a mean diameter with a Rosin-Rammler distribution parameter γ of 2.4 (same as FDS assumptions). Agent release is assumed to be instantaneous, resulting in a finite amount of liquid (typically 0.02 liter) introduced into the box at time zero. The temperature of the liquid agent is assumed to be the same as the ambient temperature. A d-squared law evaporation behavior is assumed for the individual drops with the resulting vapor instantly filling the available space. Physical properties of the agents are obtained from the DIPPR database [4].

RESULTS AND DISCUSSION

Figure 2 shows the simulation results for CF_3I at the front and aft ports when the nacelle, airflow, and discharge temperatures are the same (22 °C or -40 °C; results are plotted with different y-scales). Time zero corresponds to the initiation of agent discharge into the nacelle. The agent vapor quickly arrives at the front port since this port is located very near one of the discharge nozzles. There is a transport delay for the agent vapor to the aft port. The peak vapor concentration is higher at 22 °C than that at -40 °C and is higher at the front port than that at the aft, irrespective of the ambient temperature. At any given time, the vapor concentration is also higher at 22 °C than that at -40 °C because the evaporation of the liquid agent depends on the ambient temperature; the higher the ambient temperature, the faster the agent evaporates, resulting in higher vapor loading.

Figure 3 shows intermediate agent behavior at the front and aft ports when discharged at 22 °C (or -40 °C) into a nacelle with airflow at -40 °C (or 22 °C). For the drop size distribution used, the simulation indicates that there is a slight improvement in agent vapor loading when the cold agent is discharged into a warm nacelle, compared to a warm agent into a cold nacelle.

The results for CF_2Br_2 at the front and aft ports when the nacelle, airflow, and discharge temperatures are the same (either at 22 °C or 0 °C) are shown in Figure 4. The peak vapor concentrations in the two cases do not differ significantly. However, the arrival times of agent vapor to the two ports differ for the two conditions considered. The simulated peak agent concentrations at the two ports are a factor of two or more higher than the experimental values [5]. This is likely due to the small median drop size (20 μm) assumed in the calculations. Smaller drops evaporate faster and should result in a higher vapor loading. A median drop size of 20 μm may not be achievable for a high boiling-point agent discharged from an open tube configuration used in the experiments without a nozzle to assist atomization of the liquid agent. Figure 5 illustrates the effect of drop size on the vapor loading under the same condition.

Simulation results show that an increase in drop size results in a decrease in vapor concentration, which is expected due to a reduction in drop surface area for a given drop mass loading.

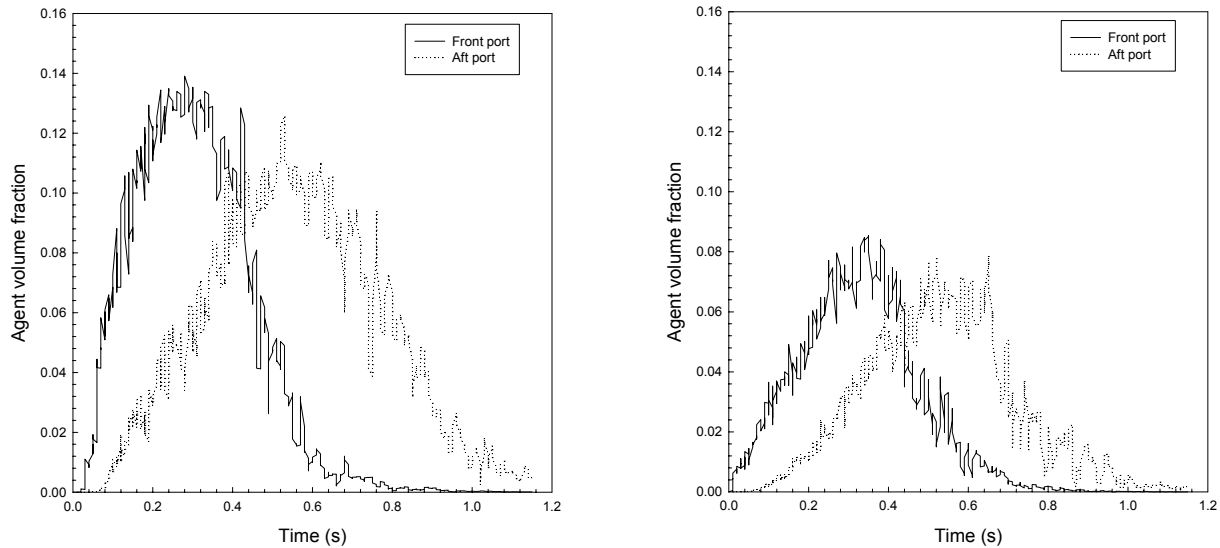


Figure 2. Simulated results for CF_3I at the front and aft ports when the nacelle, airflow, and discharge temperatures are the same. The left and right figures correspond to conditions at 22 °C and -40 °C, respectively.

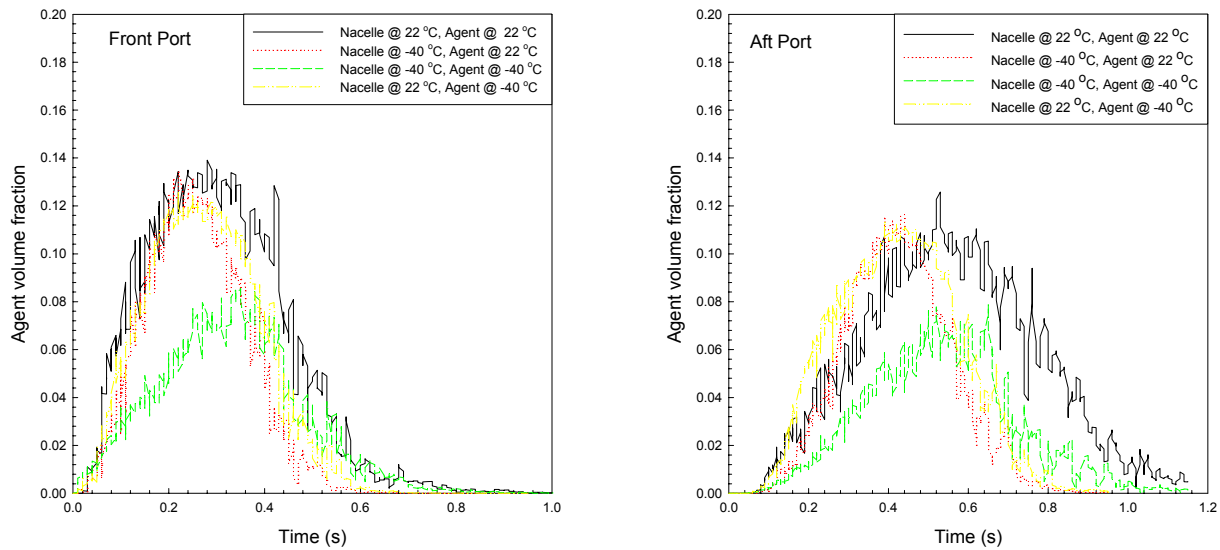


Figure 3. FDS simulation results for CF_3I at the front and aft ports for the indicated nacelle and discharge temperatures conditions.

Figures 6 and 7 show the effect of median drop size on the vapor loading at the two measurement ports for 0 °C and 22 °C, respectively. The results for 20 μm (not shown) and 200 μm drop sizes are similar, that is, the vapor loading at the front port is higher than that at the aft. However, a reversal is noted at 0 °C (see Figure 6) when the median drop size increases to 500 μm . It is

unclear if this observation is real or is an artifact of the simulation. It is plausible that under these conditions, the drop evaporation time is longer than the transport time to the front port; therefore, the vapor loading resulting from drop evaporation is low. In reaching the aft port, the drops have more time to evaporate as they are transported downstream, potentially resulting in higher vapor loading at that location. The slower evaporation rate would also explain the lower peak vapor loading from 500 μm drops than that from 200 μm drops, and the observation that it takes a longer time for 500 μm drops to attain the peak vapor loading at the same location.

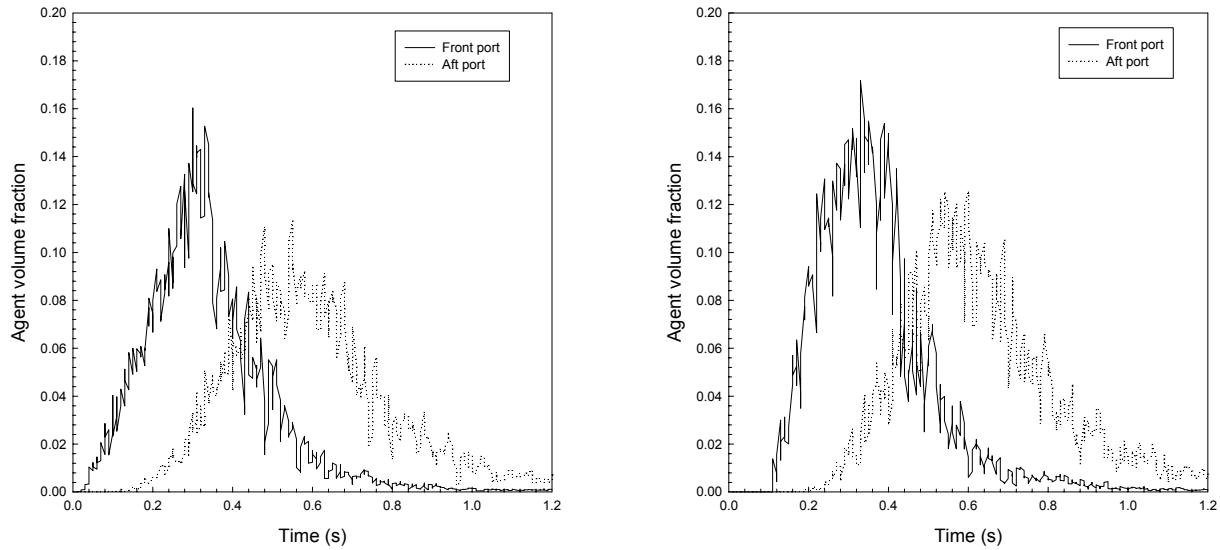


Figure 4. FDS simulation results for CF_2Br_2 at the front and aft ports when the nacelle, airflow, and discharge temperatures are the same. The left and right figures correspond to conditions at 22 °C and 0 °C respectively.

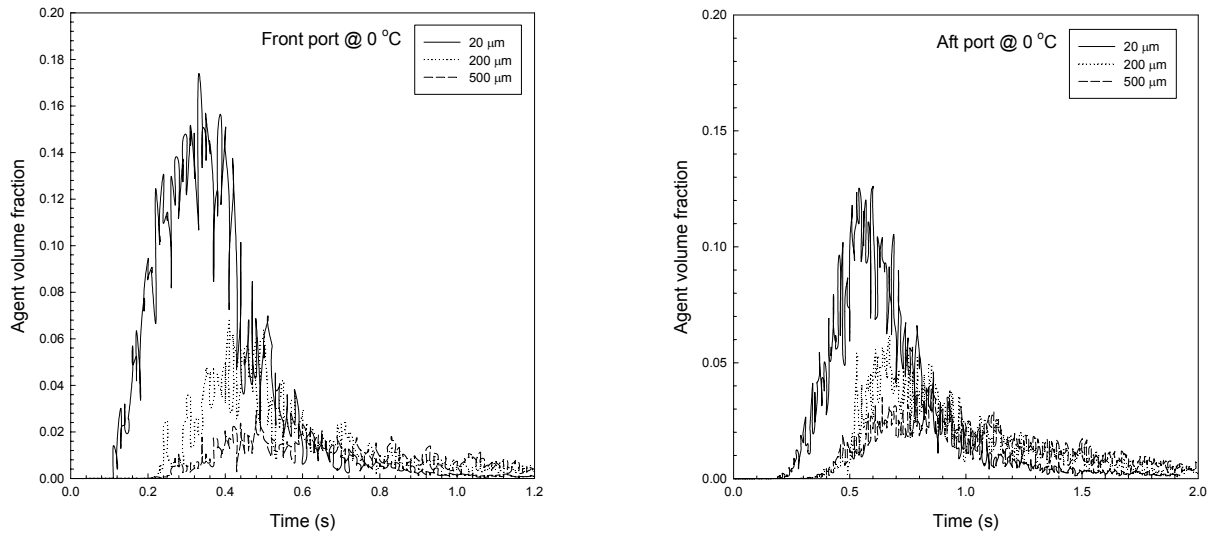


Figure 5. Median drop size effect on CF_2Br_2 vapor volume fraction at the front and aft ports. FDS simulation was performed with the nacelle, airflow, and agent all at 0 °C.

The concentration behavior in Figure 6 could also be an artifact of the simulation. The code does not have the capability to treat pooling of liquid agent and its subsequent convective evaporation from the pool in the nacelle bottom. If the drops approach a surface vertically, they are removed from the computational domain and treated as losses. Thus, less agent is present in the subsequent evaporation calculations. For 500 μm drops and at 0 $^{\circ}\text{C}$, significant liquid pooling is expected. At 0 $^{\circ}\text{C}$, liquid pooling was observed in the ELEFANT experiments although drop size distribution was not measured. The code also does not have the ability to handle drop breakup resulting from high momentum impact on the nacelle boundaries or walls due to high-pressure agent discharge. This would invariably affect subsequent drop evaporation and transport.

Figure 8a1 and 8b1 present modeling results for CF_2Br_2 released instantaneously into an empty box under similar assumptions as for the FDS simulations of Figures 6 and 7. The horizontal lines in each plot indicate the saturation limit of the vapor for the indicated ambient temperature. As expected, the saturation value limits the maximum amount of agent vapor achievable in the box for ambient temperatures below the agent boiling point. Comparison of Figure 8a1 with 8a2 for 200 μm median diameter drops and Figure 8b1 with 8b2 for 500 μm drops shows that the rate at which the agent vapor concentration approaches the saturation limit depends very strongly on the size distribution of the drops and the total amount of liquid originally introduced into the box. Under these conditions, increasing the median diameter by a factor of 2 $\frac{1}{2}$ (same spread of 2.4) has a similar effect as increasing the liquid volume by a factor of five for ambient temperatures below the boiling point (296 K for CF_2Br_2). Above the boiling point where flash vaporization is possible, the amount of liquid released clearly dominates the vapor concentration achievable. Evaluation of the effect of drop size distribution on temporal development of the vapor concentration lends support to the conclusion that the FDS concentration results presented in Figure 6 are size related. Under these conditions and time scales, the evaporation rate of the 500 μm mist competes with the convection time of the agent in the nacelle and could result in the observed higher vapor concentration at the aft port.

The cup burner value for CF_2Br_2 extinguishing an n-heptane flame is 2.6 volume % [6] (0.0012 moles/L at 273 K). It is interesting to note in Figure 8b2 that the vapor concentration for the evaporating 500 micrometer CF_2Br_2 drops released at the lower agent discharge rate into ambient temperatures colder than the boiling point do not achieve the cup burner extinction concentration even after three seconds. The cup burner value is achieved by the finer aerosol (reduction of 2 $\frac{1}{2}$ in the median diameter from 500 μm to 200 μm). The cup burner value is also achieved for the 500 μm mist by increasing the amount of agent dispersed by a factor or five. Agent weight is often the major limiting consideration for designing suppression systems. Thus, an agent delivery system design change to effect a modest drop size reduction for the dispersed agent might be more cost effective than designing for an increased amount of agent.

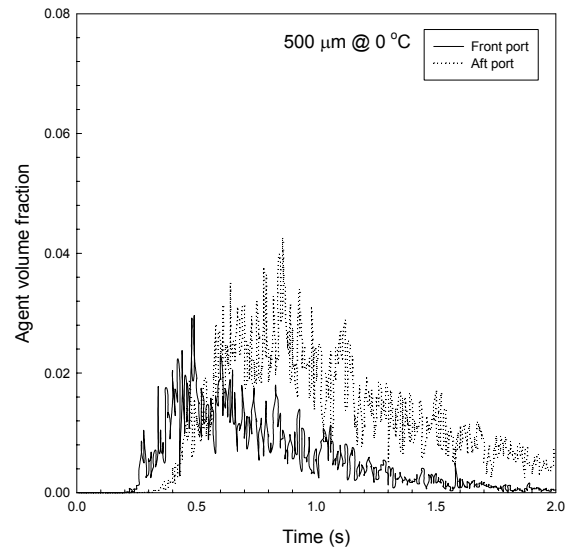
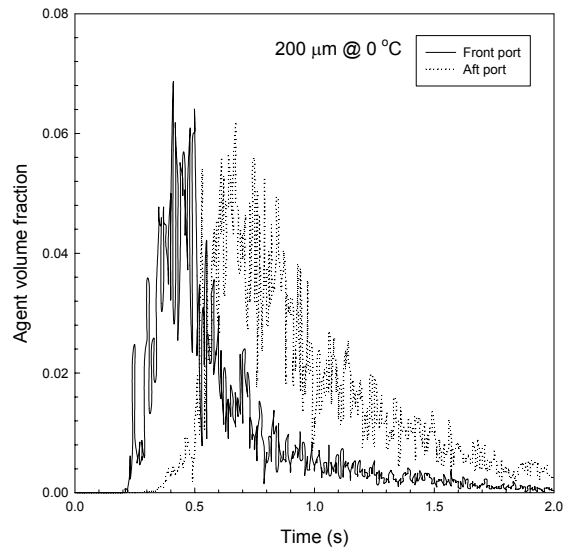


Figure 6. Effect of median drop size on CF_2Br_2 vapor loading at the two measurement ports at 0 °C.

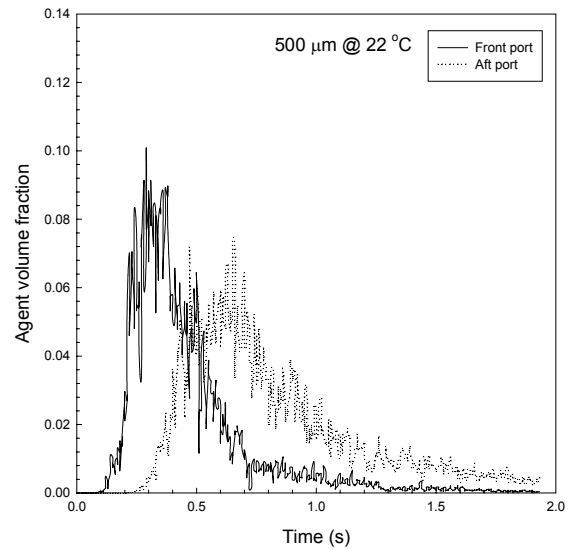
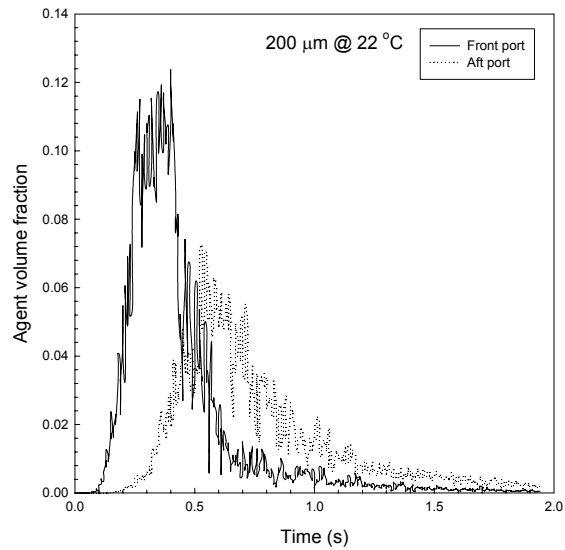
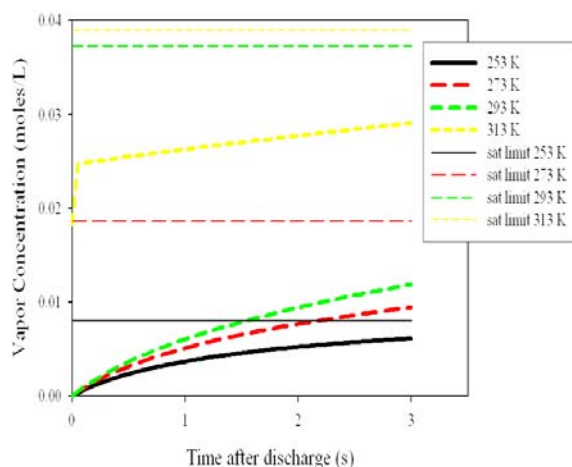
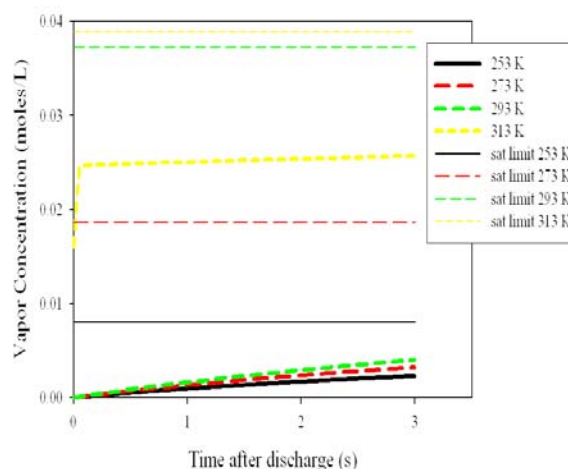


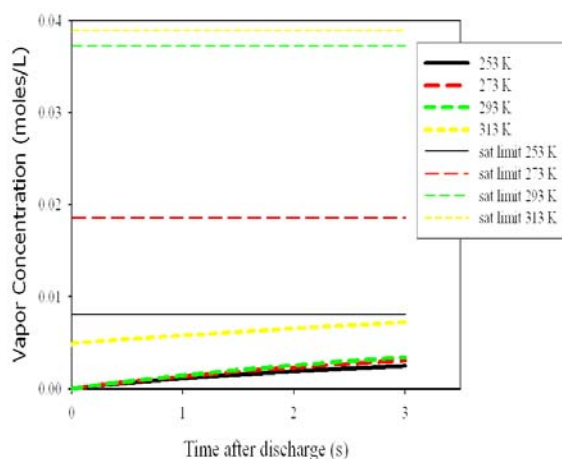
Figure 7. Effect of median drop size on CF_2Br_2 vapor loading at the two measurement ports at 22 °C.



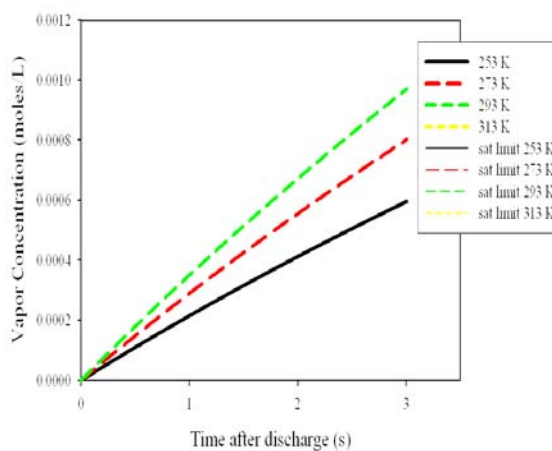
(a1)



(b1)



(a2)



(b2)

Figure 8. Concentration of CF_2Br_2 vapor following discharge of the liquid into a 0.7 L chamber with the indicated ambient air temperature. The model assumes that the agent forms a mist of drops of the unflashed liquid distributed in a log normal distribution with a spread of 2.4 about a median diameter of (a) 200 micrometers and (b) 500 micrometers. Figures 8a1 and 8b1 are for 18.75 mL total liquid (0.29 moles/L at 293 K). Figures 8a2 and 8b2 are for 3.75 mL CF_2Br_2 (0.058 moles/L at 273 K). Horizontal lines indicate the vapor saturation level at the indicated temperature. Figures 8a1, 8a2, and 8b2 are on the same concentration scale, which is 33 times that of Figure 8b2.

CONCLUSIONS

Based on Fire Dynamics Simulator modeling calculations using two agents with very different normal boiling points, we conclude that FDS can capture some of the overall *qualitative* features of agent dispersion and vapor loading in a complex nacelle geometry under various ambient conditions. More studies are needed to develop systematic trends with regard to agent physical properties. However, drop evaporation modeling in a simple geometry, combined with the FDS simulated nacelle results to date point to some general conclusions. For a fixed amount of agent dispersed into any ambient temperature, higher agent concentrations are favored by a) higher ambient temperatures and b) smaller aerosol drops. For ambient temperatures near or greater than the agent boiling point, the total amount of liquid agent dispersed dominates the vapor concentration achievable. For dispersal into ambient temperatures below the agent boiling point, the achievable vapor concentration will be limited by the saturation concentration of the agent at the ambient temperature. At a fixed ambient temperature below the boiling point, higher rates of vapor production and higher ultimate vapor concentrations are favored by a) increased total liquid agent dispersed and b) smaller aerosol drops.

These generalizations are dictated by the system thermodynamics. Quantitative predictions of the vapor temporal development must also consider the dynamics of the agent release, drop dynamics and transport, ambient flow conditions, and nacelle geometry. The spray parameters (drop size and velocity distributions, spray angles) and thermophysical property estimation used in FDS require better characterization through experimental measurements. The lack of treatment for drop impact dynamics and pooling of liquid agent and subsequent pool evaporation requires caution in the interpretation of the simulation results. In addition, highly flashing agents pose numerical instability problems for FDS depending on how the computational domain is meshed. Even with these current limitations, FDS simulations may prove to be a useful screening tool for a rapid assessment of the potential fire suppression capability due to agent vapor loading.

ACKNOWLEDGEMENTS

The authors would like to thank Dr. Kevin McGrattan of NIST for helpful discussion regarding the use of FDS code, I. Tendick of NRL for assistance in the FORTRAN coding, and Dr. Anthony Hamins of NIST for reviewing the manuscript. This work is supported by the Strategic Environmental Research and Development (SERDP) Next Generation Fire Suppression Program (Dr. Richard Gann, Program Manager) and by the Office of Naval Research (ONR) through the Naval Research Laboratory core funding.

REFERENCES

1. Fleming, J.W. and Yang, J.C., "Modeling Study of the Behavior of Liquid Fire Suppression Agents in a Simulated Engine Nacelle," *Proceedings of the Halon Options Technical Working Conference*, Albuquerque, NM, 4-6 May 2004.
2. McGrattan, K.B., *et al.*, "Fire Dynamics Simulator (Version 4): User's Guide", NIST Special Publication 1019; July 2004.
3. Yang, J.C., Manzello, S.L., Nyden, M.R., and Connaghan, M.D., "Discharge of CF3I in a Cold Simulated Aircraft Engine Nacelle," *Proceedings of the Halon Options Technical Working Conference*, Albuquerque, NM, 30 April-2 May 2002.
4. Design Institute for Physical Properties, American Institute of Chemical Engineers, 3 Park Ave, New York, N.Y., 10016-5991, U.S.A. <http://www.aiche.org/dippr>
5. Yang, J.C. and Manzello, S.L., personal communication, 2005.
6. Hamins, A.; Gmurczyk, G. W.; Grosshandler, W. L.; Rehwoldt, R. G.; Vazquez, I.; Cleary, T. G.; Presser, C.; Seshadri, K., "Flame Suppression Effectiveness", Ch 4 in Evaluation of Alternative In-Flight Fire Suppressants for Full-Scale Testing in Simulated Aircraft Engine Nacelles and Dry Bays, Grosshandler, W. L.; Gann, R. G.; Pitts, W. M., editors, NIST SP 861; April 1994, pp. 345-465.